D4.1 CALIBRATION SOFTWARE FOR HIGHER - RESOLUTION DIELECTRIC RESONATOR IMAGING OF LARGER - SCALE FILM SAMPLES AND A DATABASE OF REFERENCE DATA IN GWYDDION FORMAT

Contractual delivery date:	M12
Actual delivery date:	M12

DOCUMENT INFORMATION

Version	V6	**Dissemination level**	Public
Editor	Malgorzata CELUCH - QWED		
Other authors	Wojciech GWAREK and Andrzej WIECKOWSKI - QWED		

PROJECT INFORMATION

Grant Agreement n°	761036
Dates	1st November 2017 – 31 October 2020

DOCUMENT APPROVAL

Name	Position in project	Organisation	Date	Visa
G. Dambrine	Coordinator	IEMN		

DOCUMENT HISTORY

Version	Date	Modifications	Authors
V7			
V8			

TABLE OF CONTENT

1 EXECUTIVE SUMMARY

1.1 Description of the deliverable content and purpose

Dielectric resonators (DRs) are one of the three microwave macroscopic material measurements technologies, considered and further developed within the MMAMA project. The **main purpose** of this Deliverable D4.1 is to propose a new software technique for **enhancing the resolution** of DR measurements without the need to reduce the DR's head and increase the operating frequency. The Deliverable contains:

➢ a **brief review of inherent limitations** of DR measurements, in terms of sample size and spatial resolution, as well as earlier approaches for their overcoming,

➢ **field - theoretical derivation of a new technique** for resolution enhancement, by calibrating the raw scan of material surface with pre-simulated electromagnetic (EM) field patterns in the DR (from the modelling in WP3),

➢ **measurement and calibration workflow** implementing the proposed technique,

➢ "**virtual laboratory**" in Matlab environment, with testing models and procedures for validation of the workflow,

➢ **example results** for virtual and real - life samples.

Besides the main purpose of enhancing the DR measurements *per se,* it is believed that the concept of resolution improvement by de-embedding raw measurements with known (pre-simulated) EM field patterns **helps bridging the gap between the macroscopic and microscopic measurement technologies** considered in the project.
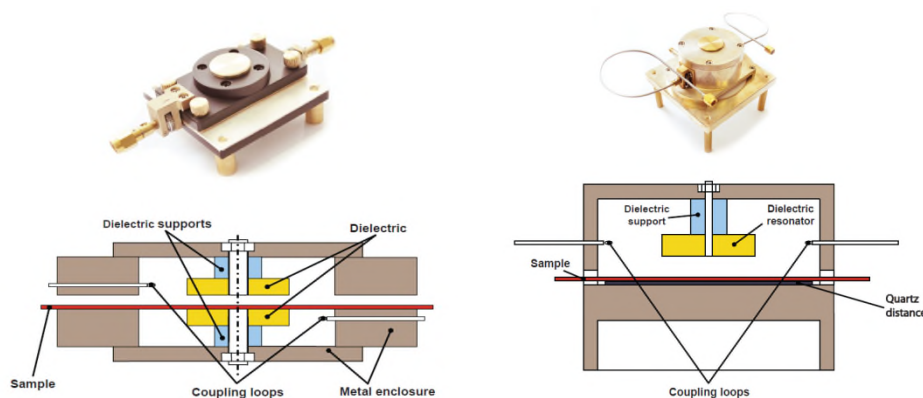

Fig. 1: Split-post and single-post dielectric resonators by QWED, for which a resolution enhancement technique is proposed in this Deliverable.

1.2 Brief description of the state of the art and the innovation breakthroughs

Dielectric resonator methods based on split-post (SPDR, Fig. 1 left) and single-post (SiPDR, Fig. 1 right) resonator configurations are a **well-established and accurate technique** for material measurements at microwave frequencies. The measurements are non-destructive and easy to perform: planar samples are inserted without any dismantling of the resonator and each resonator needs to be calibrated only once, upon manufacturing. The SPDR method

3

is commonly considered the most accurate one in the measurements of permittivity and loss factors (especially of low-loss materials). It is an industrial (and a formal IEC) standard.

What restricts the application of DRs to materials containing nanoparticles or thin-film stacks such as solar cells, is their limited resolution. Each DR provides complex permittivity of the material averaged under the DR's "head". At a nominal frequency of 10 GHz the averaging area should be considered as ca. 16 mm in diameter (or at least 8 mm with ca. 90% accuracy). While theoretically the spatial resolution increases linearly with the increase of frequency, such an approach is impractical due to high complexity (and hence prohibitive costs) of manufacturing and calibrating the resonator. The family of SPDRs readily available at an acceptable price of a few kEUR terminates at 15 GHz with ca. 12 mm effective resolution.

In Task 4.4 we have now proposed and evaluated the possibility to downscale the DR measurements without reducing the geometrical size of the DR's "head" or increasing the measurement frequency. To begin with, we took advantage of the micro-scale insight into the electromagnetic quantities and phenomena within the DR, as facilitated by QuickWave EM software and exploited within WP3. We observed that the measured microwave signal is due to a geometrically weighted contribution of the material parameters, where the 2D weighting function is the squared electric field, further referred to as the DR's *template*. In principle, the *template* is obtainable with any state-of-the-art EM simulator, but QuickWave features an exceptional variety of the relevant co- and post-processing functionalities.

Our state-of-the-practice is as follows. Within **WP3**, we generate the DR's *template* by ultra-fast BOR FDTD (Bodies of Revolution Finite-Difference Time-Domain) simulations implemented in the QW-V2D version of QuickWave. Further, in **WP5** we have designed and manufactured a prototype of the 2D scanner, where a sample of up to 80 mm x 80 mm size is initially imaged in 1 mm steps (thought the applied commercial motors allow us to go down to 5μm steps). Then in this **Task 4.4**, the matrix of raw coarse measurements is transformed into the refined image, using the *template* matrix.

In this **Deliverable**, we apply our own downscaling technique based on direct matrix inversion. The inversion is shown to be ill-conditioned, and thus we need to apply numerical techniques for matrix regularisation. Nevertheless, experiments indicate advantages of our new technique, with respect to the deconvolution in the Fourier domain, which was initially considered for development in the MMAMA proposal.

1.3   Corrective action (if relevant)

N / A

1.4   IPR issues (if relevant)

Relation to Background:
The concepts of calibrating raw DR measurements into refined images of complex permittivity distributions by means of:

- extracting local field values from full-wave EM simulation by the FDTD method,
- incorporating those local values into the discretised fundamental EM equations linking resonant frequencies to energy stored in the system (and Q-factor changes to the losses)

are inherent in QWED Background Knowledge as declared in the MMAMA proposal.

Generated Foreground:

The linear matric algebra technique for downscaling the DR measurements becomes Foreground Knowledge of QWED. The concept has been proposed for presentation at MMAMA workshops (IMS and EuMW 2019) and its electromagnetic bases are planned to be explained in a regular submission to the IMS 2019 SC-33.

QWED aims to incorporate the technique into its commercial products. Publication in full is not intended. Patenting does not appear worthwhile at this stage.

Relation to third party IPRs:

Our resulting new linear matrix algebra technique is initially compared in this Deliverable to the deconvolution in the Fourier domain. The Fouried domain approach was initiated by QWED team and pursued in a Ph.D. by P. Korpas of the Warsaw University of Technology (also in "*Deconvolution-based spatial resolution improvement technique for resistivity scans acquired with split-post dielectric resonator*", MIKON 2018). Dr. Korpas holds IPRs for the Fourier domain method. He will be involved in the MMAMA activities when the two methods will further be compared and validated throughout the project.

2 PURPOSE

2.1 Outline of the methodology for resolution enhancement

Measurements of complex permittivity in SPDRs and SiPDRs are based on the fundamental relationships of resonant frequencies and Q-factor changes – to electric energy and dissipated power changes. The measurements reflect integral values of such changes over the resonator volume:

$$\frac{f_e - f_s}{f_s} = \frac{C_1}{2} \iiint\limits_{V_s} \epsilon'_{r1}(x,y) \cdot |E_e|^2 \, dV$$

$$\frac{1}{Q_s} - \frac{1}{Q_e} = C_1 \iiint\limits_{V_s} \epsilon''_r(x,y) \cdot |E_e|^2 \, dV$$

(0)

Our technique, in essence, aims to distribute energy and power changes over the resonator subdomains, and thereby to characterise each subdomain with its localised complex permittivity values. Since SPDRs and SiPDRs are applied to flat planar samples, our target is a 2D complex permittivity pattern over the sample surface.

Our reasoning is as follows:

1. Assume that we consider a two-dimensional measurement domain divided into squares (cells) of size a and that the entire domain has the size of M x N cells. Centers of the cells are placed in the nodes x=m a; y=n a, where m=1..M, n=1..N. Inside each cell we assume averaged value of the permittivity $\varepsilon(m,$n) and conductivity $\sigma(m,n)$. In the first scenario we assume for example a= 3mm, M=40, N=50 (Fig.2 marked by the blue line).

2. That domain is being moved in the slot of the SPDR and is under the influence of electric field of a specific 2D distribution. The region of SPDR (denoted by the orange colour) is divided into the same cells as the entire domain. Those cells are situated with respect to the center of the resonator (denoted by a red cross) in the positions of x= k a, y=l a, where k= -K..0..+K, l=-L..0..+L. In the first trial we can assume for example $K=L=6$.

3. In the SPDR (or SiPDR) measurements the change of the resonant frequency is proportional to the increase of the total electric energy stored in the resonator and is proportional to $(\varepsilon-\varepsilon_0)E^2$ caused by change of the permittivity introduced by the measured sample. Consider the resonator of Fig.2 where the area of maximum E-field is marked in red. Let us digitise the area of the resonator (denoted by orange color)

assuming there a constant value of ε_d of the dielectric sample. We will get the energy increase caused by insertion of the dielectric sample:

$$W_0 = a^2 h(\varepsilon_d - \varepsilon_0) \sum_{k=-K}^{K} \sum_{l=-L}^{L} E_T^2(k,l) = h(\varepsilon_d - \varepsilon_0) \qquad (1)$$

where: - h is the thickness of the dielectric sample.

- E_T^2(k,l) is the electric field of the resonator template or in other words electric field in the resonator slot averaged over the cell (k,l) with the amplitude chosen that way that equation (1) is obeyed. Thus the resonator measurements should give the normalised detuning of the resonator with a sample of the thickness equal 1 and permittivity equal to ε_d =2 ε_0 .

4. Assume that we are now measuring a sample divided into cells as in point 1. We *place the center of the resonator in the point (m,n) – for example in Fig.2, we have m*=28, *n*=10. Summation over the active surface of the resonator (the orange square) will allows calculation of the expected detuning as caused by the energy change :

$$W_{mn} = a^2 h \sum_{k=-K}^{K} \sum_{l=-L}^{L} (\varepsilon_d(m+k,n+l) - \varepsilon_0) E_T^2(k,l) \qquad (2)$$

where: - ε_d(m+k,n+l) is averaged permittivity in the cell of the marked with the index (m+k,n+l) , assuming that if m+k extends beyond the range from 1 do M or n+l extends beyond the range between 1 do N, in summation we take the value of 0.

That way we can simulate the result of "virtual measurement" giving fuzzy edges similar to those obtained in the real measurements. Fig.2 proposes the measurement domain. We have there a plate 120 x 150 mm assumed to have relative permittivity equal 2 with a rectangular insert of relative permittivity equal 4 and the size of 36 x 24 mm situated such that one corner of it touches the center of the bigger plate (red plate in Fig.2). That scenario will be used for testing the correction algorithm (with the aim of increasing the resolution of the measurements).

5. The correction algorithm is supposed to give the result which is reciprocal with respect to the one described in p.4. It means that on the base of the matrix composed of the elements W_{mn} (2) we should obtain matrix V_{mn} describing the distribution of the material properties after correction. That should correspond more closely to the real distribution of the properties of the measured sample of Fig.2. That means that assuming *h=1* the value of V_{mn} should be equal:

- 0 outside the blue plate,
- 1 in the blue plate outside the black plate,
- 3 in the area the black plate.

In the matrix *[W]* as well as in matrix *[V]* we have *P=NxM elements.* We can create *P=NxM* linear equations describing relations between the elements and after solving those equations we will obtain the corrected result of the measurements. Thus we should generate a square matrix *X* with the number of rows and columns equal to *P=NxM*. Matrices *[W]* and *[V]* can be written in a vector form :

$[W]'$=(w_{12},w_{13}..w_{1m}, w_{21},w_{22}..w_{2m}...... w_{n2},w_{n3}..$w3_{nm}$) and similarly for *[V]'*.

We aim at a relation:

$[X]\,[V]'=[W]'$ where *[X] and [W]'* are known and we need to obtain *[V]'* (3)

Matrix *[X]* is generated in a way that the element in the chosen position (row, column) denoted *x(r,s),* for each r and s is equal to :

- $E_T^2(k,l)$ for *s= r+k+ml* (for *k=-K...+K* and *l=-L...+L*)

- *0* for *s* not obeying the above condition.

It means that in each row of the matrix *[X]* we have not very many non-zero elements. For example for P=2000 and K=L=6 we have 169 non-zero elements out of 2000 in the row (filling factor of about 8.5%). In this example a relatively big resonator was assumed (of the diameter equal to 24 mm with the active area of about 36 x 36 mm). That corresponds to a real resonator for the frequency of about 5 GHz. When we assume the active area of 18 x 18 mm (corresponding to a resonator for 10 GHz) the filling factor will be reduced to approximately 2.1 % which may open a possibility to apply the sparse matrix methods for solving equation (3).
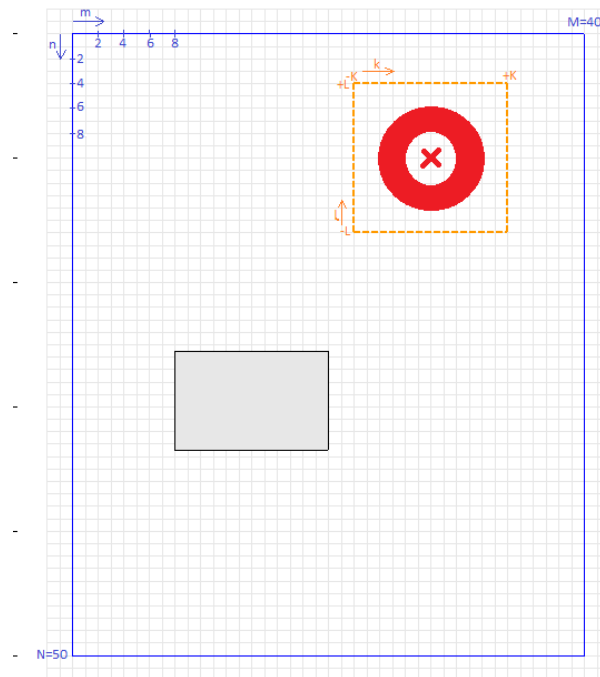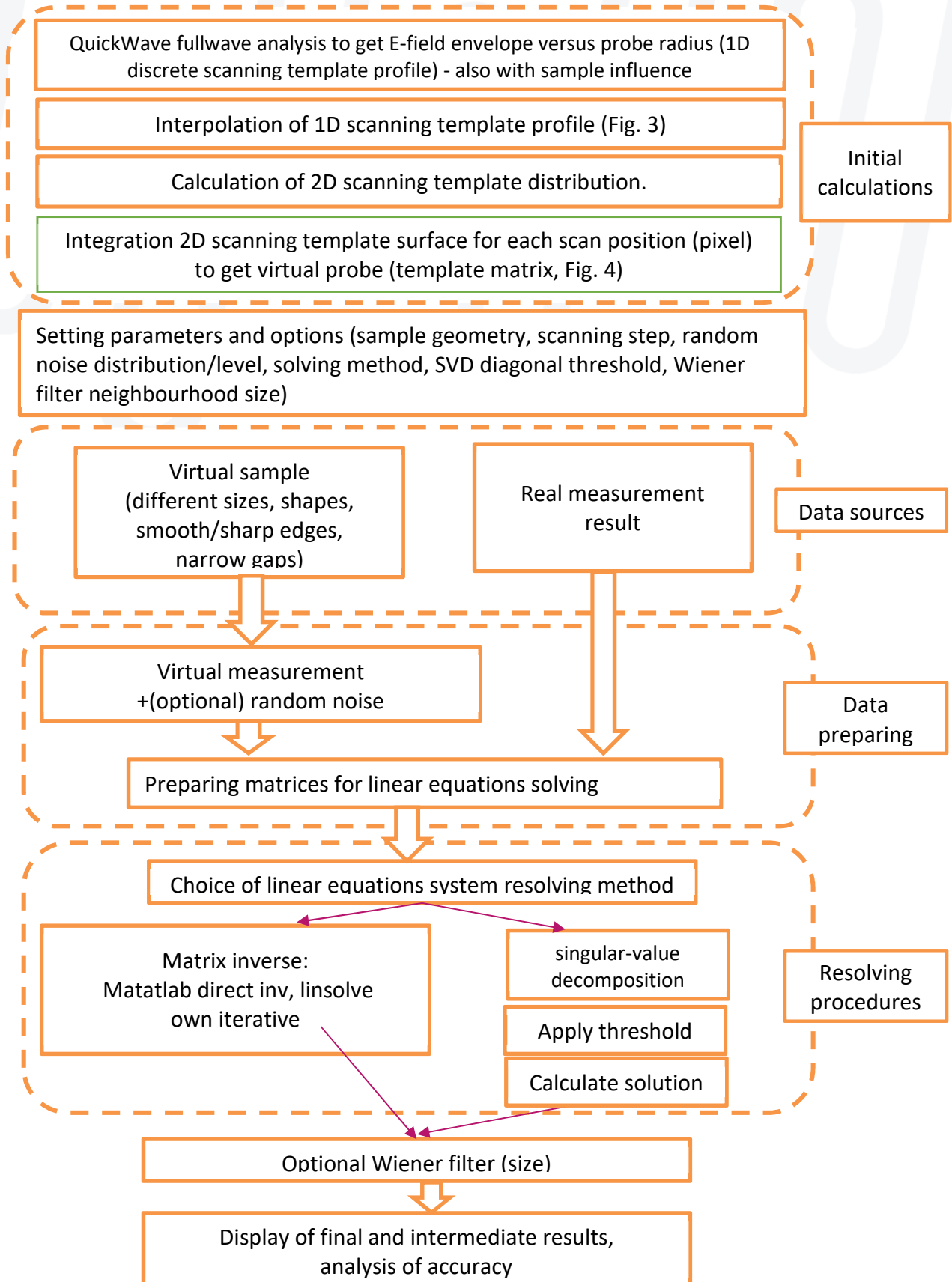

Fig.2: Measurement domain illustrating the proposed resolution enhancement technique.

2.2 Calibration workflow for higher-resolution DR imaging

The workflow of raw DR measurements followed by the new calibration technique for resolution enhancement is presented below. The first step (EM simulation of the resonator) is performed by the QW-V2D version of QucikWave software. Further steps are implemented in Matlab. The implementation forms a "virtual laboratory" for convenient testing of:
- different algorithms (e.g. matrix inversion)
- different calibration parameters (e.g. SVD threshold, Wiener filter size)
- influence of measurement noise.

8

QuickWave fullwave analysis to get E-field envelope versus probe radius (1D discrete scanning template profile) - also with sample influence

Interpolation of 1D scanning template profile (Fig. 3)

Calculation of 2D scanning template distribution.

Integration 2D scanning template surface for each scan position (pixel) to get virtual probe (template matrix, Fig. 4)

Initial calculations

Setting parameters and options (sample geometry, scanning step, random noise distribution/level, solving method, SVD diagonal threshold, Wiener filter neighbourhood size)

Virtual sample
(different sizes, shapes, smooth/sharp edges, narrow gaps)

Real measurement result

Data sources

Virtual measurement
+(optional) random noise

Preparing matrices for linear equations solving

Data preparing

Choice of linear equations system resolving method

Matrix inverse:
Matatlab direct inv, linsolve own iterative

singular-value decomposition

Apply threshold

Calculate solution

Resolving procedures

Optional Wiener filter (size)

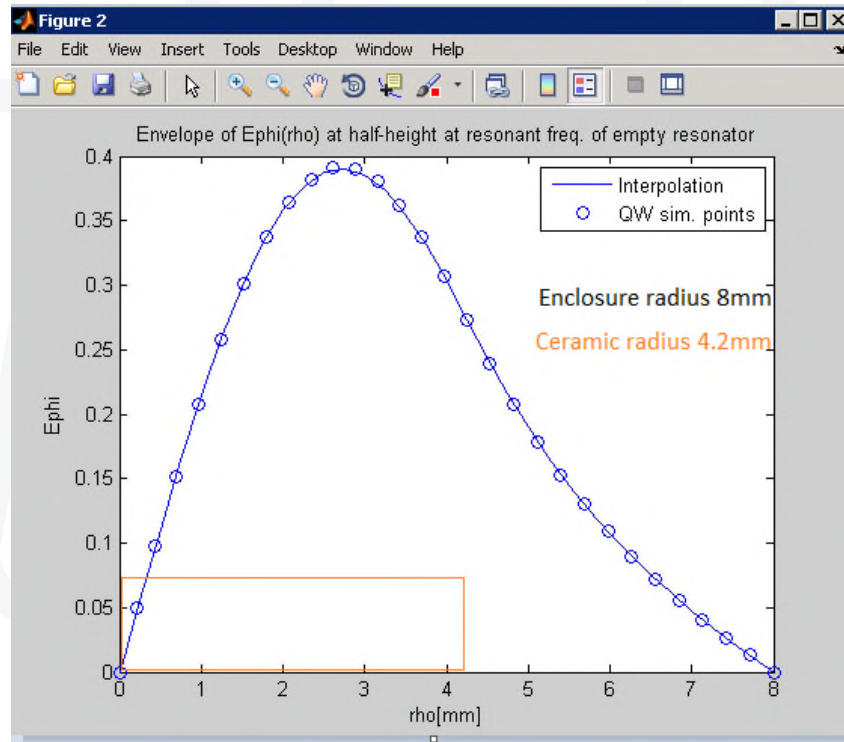Display of final and intermediate results, analysis of accuracy

Fig. 3: Radial profile of angular E-field in 10 GHz SPDR: QW-V2D simulated points and Matlab interpolation.
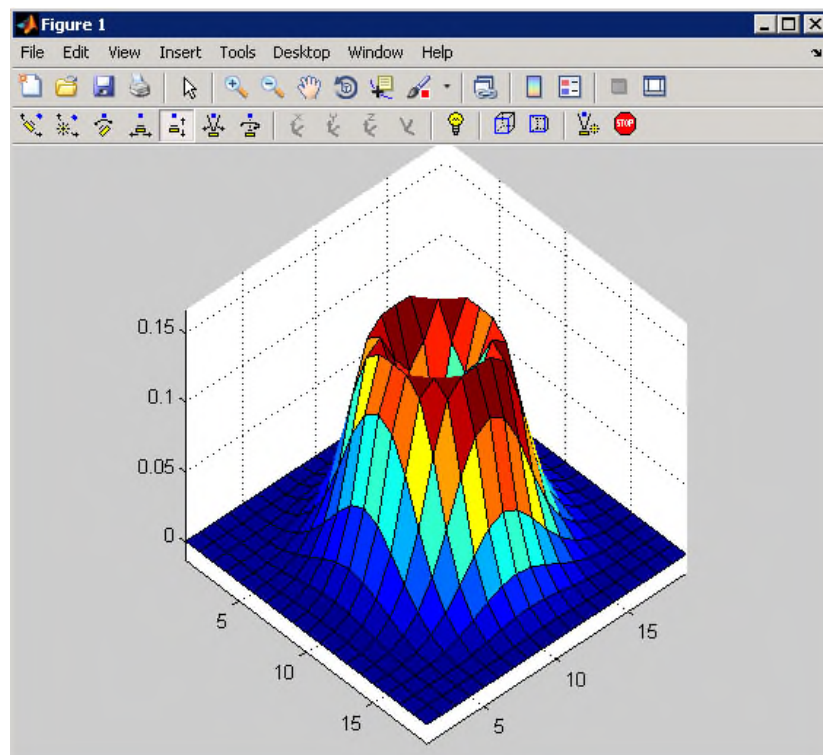

Fig. 4: Template 2D matrix in 1mm x 1mm cells, over central cross-section of 10 GHz SPDR.

2.3   Workflow validation with virtual samples

We first validate the proposed methodology with a virtual sample, which is a rectangular patch of a homogeneous material placed in air (Fig.5 left), with an additional dot of the same material. We apply a *template* that is also virtual, but retains the main features of electric field distribution in the SPDR measurement mode - it is axisymmetrical, with zero field at the centre, and the highest field concentration approximately at half-radius of the ceramic (Fig. 6).

We perform a virtual scan, assuming that the *template* of Fig. 6 is moved over the scanning region that embeds the sample (with air margins); at each *template* position over the region we integrate the electric energy over the surface. This produces a virtual scan as in Fig.5 (2nd column). In this scan, the sample is seen but with an apparent quasi-Gaussian radial inhomogeneity and a halo around its circumference, because at other than its central positions the *template* covers partly material and partly air cells. The dot was too small with respect to the *template* size, to produce a measurable effect.

To improve the resolution, we now solve the inverse problem to eq.(3). The system is sufficiently small to efficiently apply direct matrix inversion (with the method automatically selected by Matlab). Our matrix solution (3rd column of Fig. 5) restores the rectangular shape of the sample; however, because the inverted matrix was ill-conditioned, numerical round-off errors have been amplified into a spurious noise superimposed onto the expected pattern. Further however, the distortions are effectively filtered out with the Wiener filter of 7 *template* cells in size (4th column in Fig. 5).
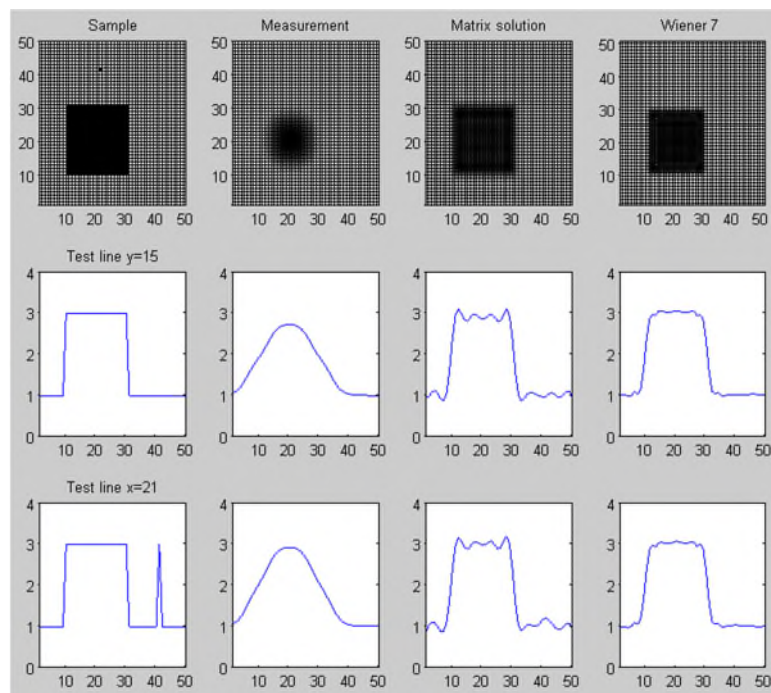

Fig. 5: A virtual rectangular sample (*Sample*, 1st column), its virtual scan with the *template* of Fig. 6 (*Measurement*, 2nd column), the scan downscaled with the same *template* using direct matrix inversion (*Matrix solution,* 3rd column), and then cleared of numerical noise by Wiener filter of 7 cells in size (*Wiener 7*, 4th column). The 1st row are 2D images, the 2nd row is a horizontal cut at half-height of the main sample, the 3rd row is a vertical cut passing through the dot of material.
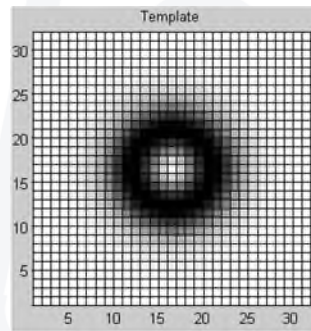
Fig. 6: Template assumed for virtual scanning – generated manually but resembling the essential features of the real SPDR template of Fig. 4.

In real-life measurements, there will be more noise than that due to numerical round-off errors. We emulate such a situation by adding a random noise of 2% to each virtual measurement of the 2nd column. This second experiment is presented in Fig. 7 and – at first sight – its 2nd column does not look worse than that of Fig. 5. However, the image after matrix inversion (in column 3) is significantly more "noisy", once again, due to error amplification by the inverted ill-conditioned matrix. After applying the same Wiener filter of size 7 there clearly remains space for improvement. Wiener filter of size 3 (lower block of displays) is clearly too weak for removing the noise.

While the above reported experiments seem encouraging, they are not fully representative of our early experiments conducted during the first 6 months of the project. In fact, we were observing quite an erratic behaviour of the technique, for different meshing of the same sample and the same template. For many meshing, the system was sill-conditioned but in some cases the determinant was further dropping by many orders in magnitude. We were trying different direct methods of matrix inversion in Matlab and also implementing our own iterative methods, in a quest to gain more control over the numerical system, but unsuccessfully.

It was only a deeper academic re-visiting of the linear matrix algebra that brought us to a stable solution, which resides in the so-called matrix regularisation. In short, instead of trying to invert the ill-conditioned matrix, we perform its Singular Value Decomposition (SVD in Matlab) and replace the smallest (trouble-causing) eigenvalues by precise zeros. In fact, only 10-30% of non-zero eigenvalues need to be typically retained for a consistent performance of our resolution improvement technique. Example results are given in the following Section.
In cases that could be treated by direct or iterative matrix inversion (as in Figs. 5 and 7), the results of the SVD approach remain similar. The advantage of the SVD approach is, that it works reliably and well reproduces the original image irrespectively of spatial meshing and also in the presence of high numerical noise.

A new task for further WP4 activities is optimisation of the number of eigenvalues to be retained, for different types of permittivity distributions.
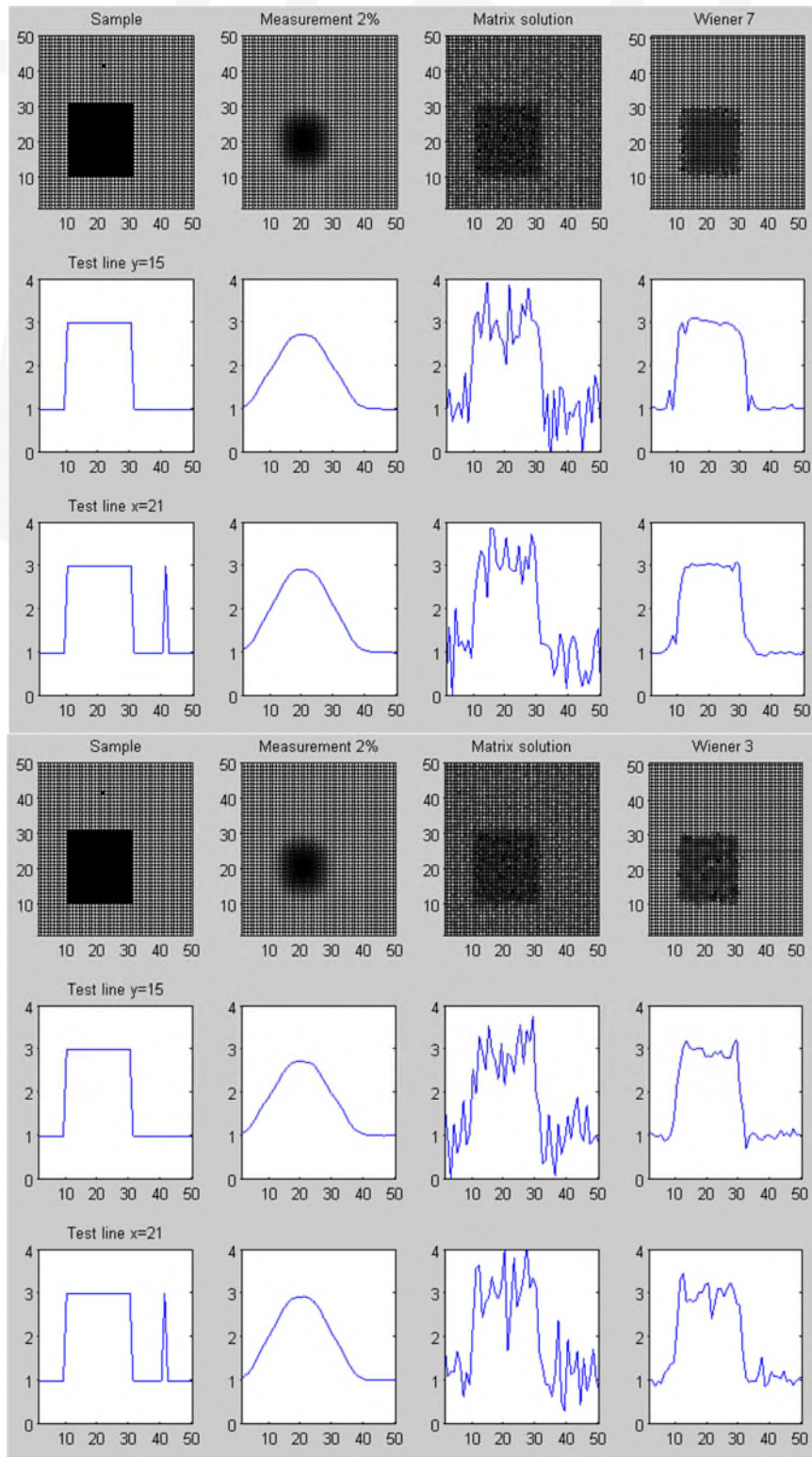
Fig. 7: The experiment of Fig. 5 with random 2% noise added to the virtual measurement in the 2nd column: effects of Wiener filter of different size (7 in the upper and 3 in the lower block of displays).

2.4   Resolution enhancements of real-life samples and scans

In the MMAMA proposal it was assumed that a number of real-life scans would be available for the validation of our enhanced-resolution imaging algorithms fom the database created in a parallel activity at the Warsaw University of Technology (WUT). Unfortunately, this has not been the case: mechanical operation of WUT scanners has not been sufficiently stable in automatic mode and the only raw images we have been able to use have been those produced semi-manually in the Ph.D. work of P.Korpas.

Fig. 8 shows an example result from the aforementioned Ph.D. thesis, while Fig. 9 shows the results of our techniuqe, applied to the same raw measurement. Visually, our technique better restores the rectangular shape and is free of quasi-circular reconstruction artifacts ("waves" in the picture), that in the method of Fig. 8 can be attributed to the globalisation of local errors by Fourier transform. However, we also note that visual criteria may be too arbitrary for comparing the two methods. Quantitative criteria for the quality of permittivity reconstruction will need to be formulated further in the project.

There is also one curiosity in our restored image (columns 3 and 4 in Fig. 9): it indicates a glitch in the manual measurement process, probably incidental folding of the foil on which the sample was mounted, during the scanning.

Finally for this sample, we have tried applying our technique with a coarser 5x5 template (obtained from that in the right picture of Fig. 9 by summing up cell clusters). The glitch due to the (deduced) foil folding is hidden by averaging, but the template is clearly too coarse to reconstruct the rectangular shape.
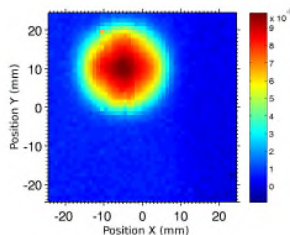

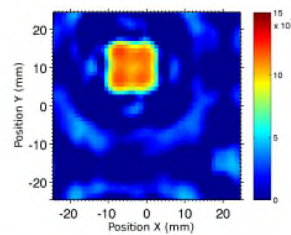Fig. 1. Measured loss tangent on 10x10 mm sample of FR4 substrate.

Fig. 2. Measured loss tangent on 10x10 mm sample of FR4 substrate (after reconstruction).

Fig. 8: Results from the Ph.D. thesis of P.Korpas (WUT): raw image of a rectangular sample obtained with 5 GHz SPDR and the result of resolution enhancement by deconvolution in Fourier domain.
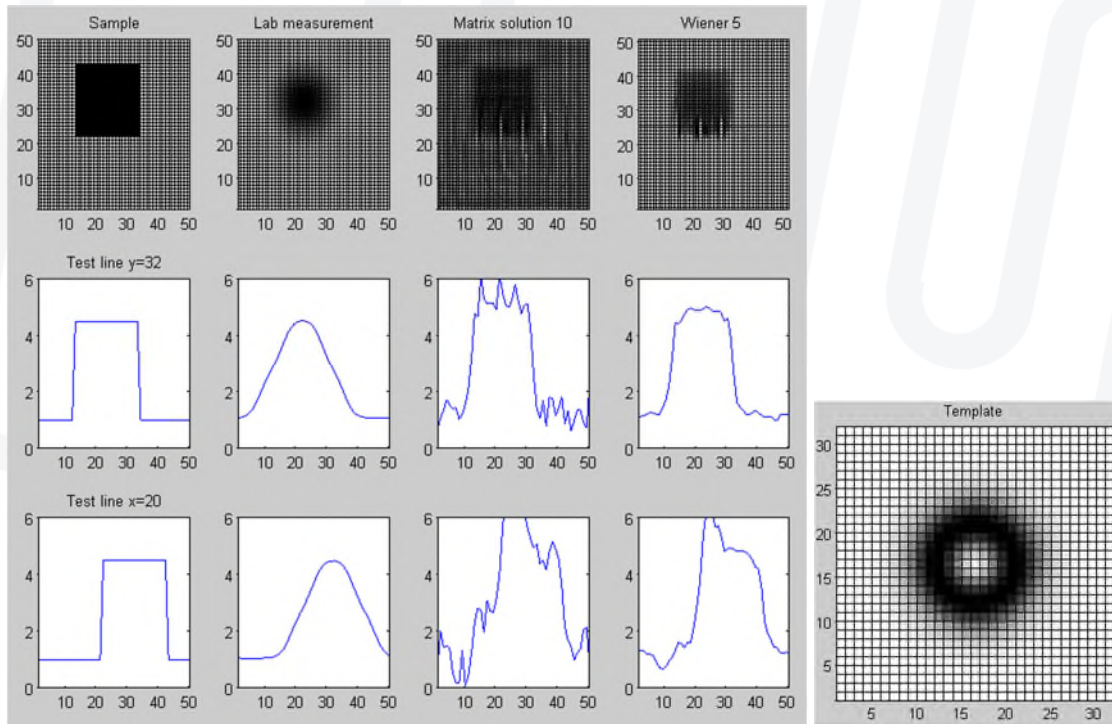
Fig. 9: Our resoluiton improvement technique applied to the example of Fig. 8. In consecutive columns of the left picture we see : real sample, raw measurement (the same as the left picture of Fig. 8, tabulated data courtesy of P.Korpas), resolved image after matrix solution, and the final image after Wiener filtering. The right picture shows a 31x31 tempolate created with QW-V2D (BOR FDTD) software for the computational model of QWED 5 GHz SPDR.
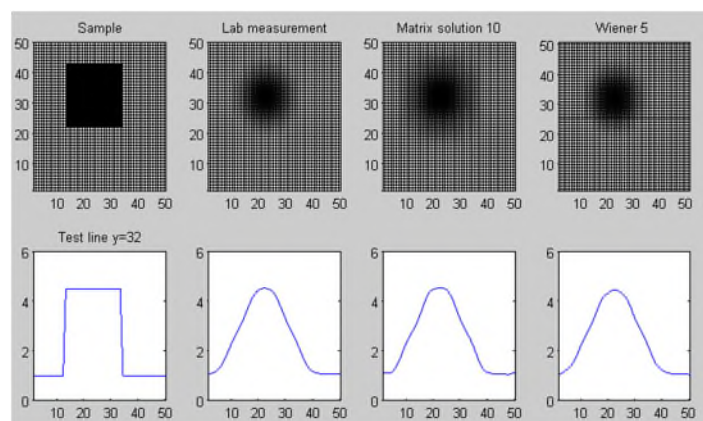

Fig. 10: Resolutioon improvement experiment as in Fig. 9, but performed with 5x5 template.
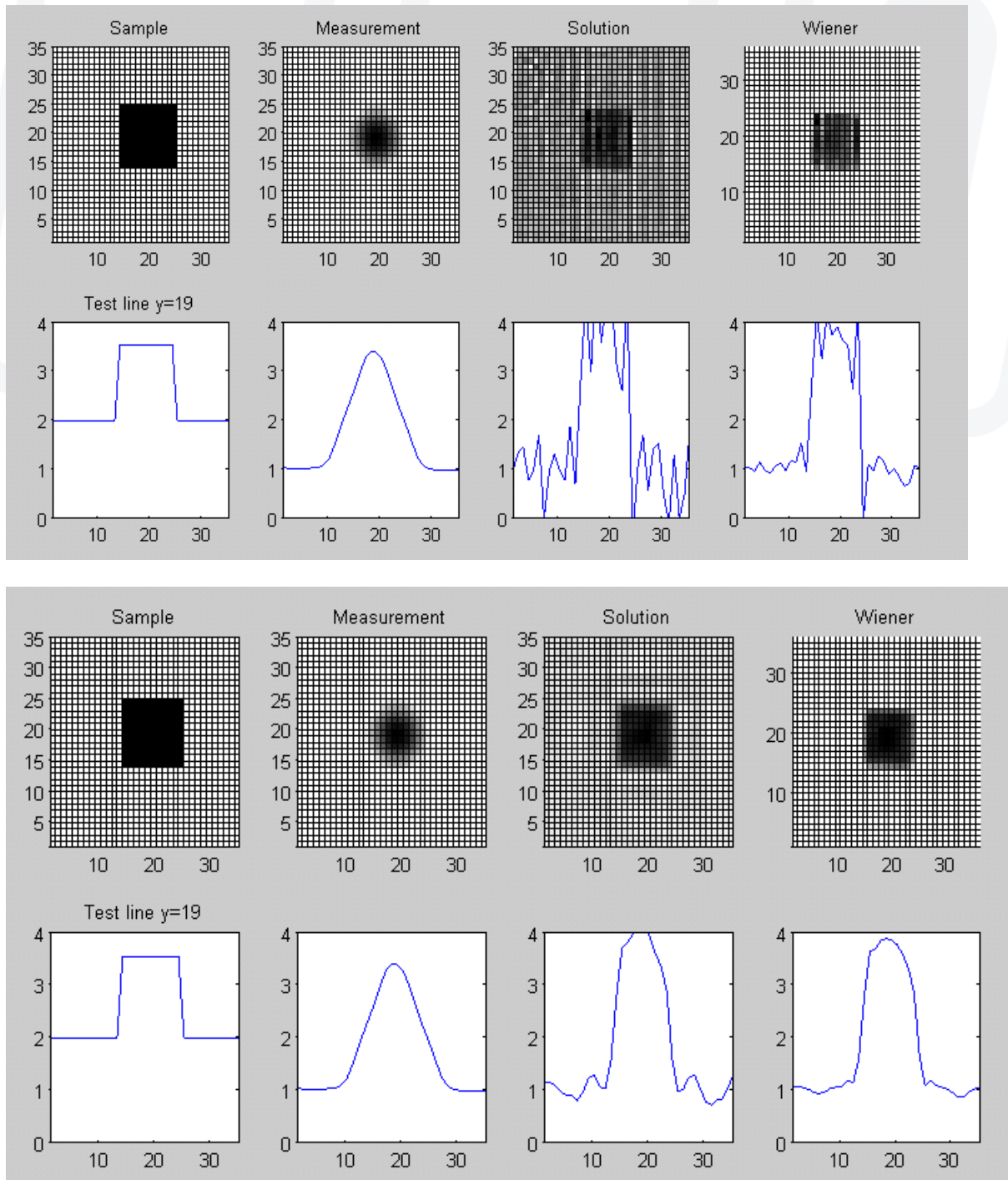
Fig. 11: Results for a real-life sample (visualised in the 1st column), for which a 1mm resolution scan (2nd column) has been obtained by QWED new 10 GHz SPDR scanner (constructed in WP5). The *template* for the SPDR has been produced in WP3 (and shown in Figs. 3 and 4). After SVD, either 30% (upper block of images) or q0% (lower displays) of eigenvalues are retained in the solution of column 3.

2.5 QWED approach to Gwyddion format implementation

Following the MMAMA proposal, results of all virtual and real-life measurements as well as EM simulations will be stored in a Gwyddion-compatible format and made accessible through the Open Innovation Environment. The actual formats for data storage are being decided in WP6.

Thus as the first step, QWED software engineers have ensured that the files saved by QuickWave software can be read with Gwyddion software available to us. This is exemplified in Fig. 12, where S-parameters of a standard waveguide-to-coax transition are presented first in QW-Simulator, and then in Gwyddion 2.49 Viewer.

In a manner similar to Fig. 12, frequency-domain characteristics and modal *templates* of SPDRs (as used in this D4.1) can be handled, as the initial solution to the Gwyddion requirement. For the WP Leaders teleconference in October 2018 QWED posed a question about the final formats for modal templates (from simulations) and scanning results (from measurements and calibration post-processing). Further instructions have been received from METAS and are currently being implemented.
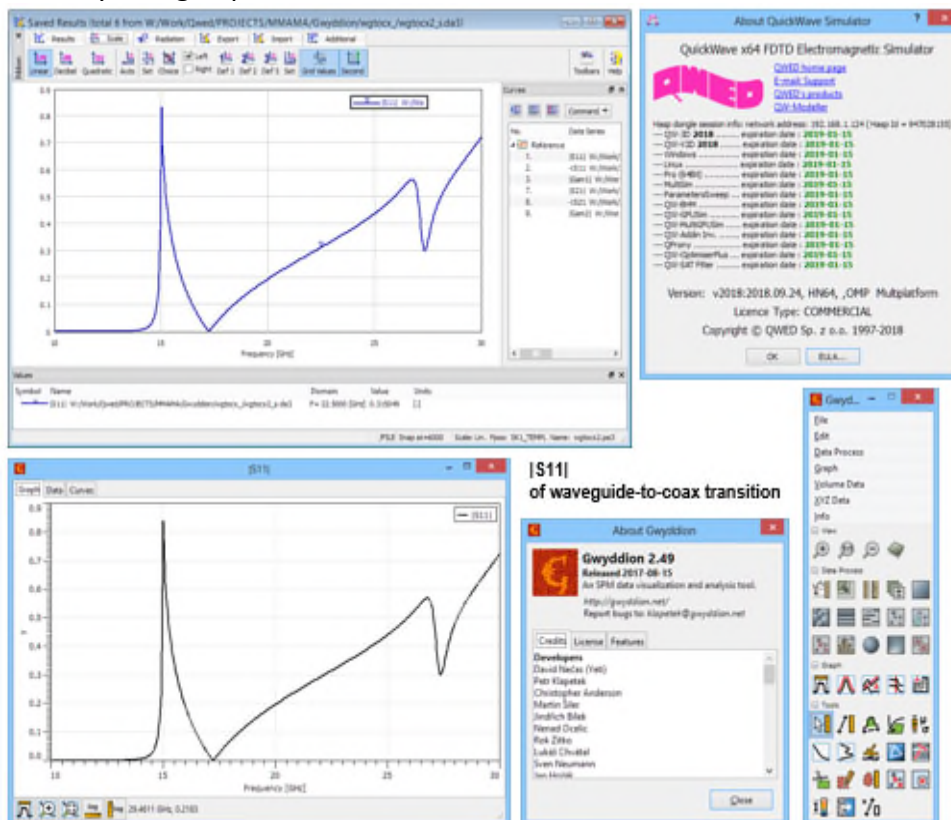

Fig. 12: Simulation results of the QuickWave standard example (waveguide to coax transition): upper – displayed directly in QW-Simulator (and subsequently saved to a text file); lower – displayed in Gwyddion Viewer.

3   CONCLUSIONS

The overall result reported in this Deliverable is a Matlab implementation of the proposed DR measurement and calibration workflow, including our new resolution enhancement technique. This forms a **"virtual laboratory"** for further developments of the calibration workflow and optimisation of both electromagnetic and computational parameters, including:

- scanning step of the raw measurement,
- spatial resolution of the *template*: both at the simulation and interpolation stages,
- threshold of singular value decomposition of the system matrix,
- noise filtering parameters,
- (possible) adaptive *template* deformation to account for technological deviations between the actual DR and its EM model assumed in WP3,
- conditions for the *template* generation: fixed for a particular DR or initially adjusted to account for the presence of each sample,
- definition of accuracy criteria (goal functions) for permittivity image reconstruction,
- parameter -sweep and optimisation routines for reconstruction improvement.

A compromise will need to be made between EM fidelity and numerical errors: refined discretisation of the *template* combined with a refined scanning step theoretically facilitate better localisation material inhomogeneities, but lead to quadratic increase of matrix sizes and deteriorate its conditioning. Moreover, long computing times of large matrix systems will become unacceptable for industrial in-line use.

It is expected that optimum parameters may be sample-dependent. For example, increased size of Wiener filter better removes measurement noise in the case of continuous permittivity profiles, but dilutes sharp material sample edges. Further studies will only be possible after full automation of our 2D scanner prototype (in WP5) and delivery of an adequately wide range of practical samples from the partners (throughout this WP4).

Last but not least, industrial implementation of the technique must be addressed. It implies that not only must the technique work reliably and accurately, but is must also be sufficiently fast. Therefore, after further testing the technique and optimising its parameters in the convenient Matlab environment, its C++ implementation will be undertaken.

4   ANNEX 1

MMAMA_D4_1_mfiles.zip contains the Matlab files constituting our "virtual laboratory" for implementing and testing the calibration software for resolution improvement over large samples scanned with a dielectric resonator.
This annex remains confidential.

Components used by other modules:
- read_de3 - reads de3 file (QuickWave Ephi envelope result)
- Er - defines interpolation function Ephi versur radius needed for integral procedures
- //r_curve - procedure for Bessel functions test (for tests with virtual examples and analytical template)
- readscan - reads scan results from the first real measuments (discrete)
- resol - test function using inverse matrix method (for method inv)
- templmode - angular expansion of Er (necessary for calculation 2D template with templN function)
- templN - calculates 2D template (size NxN) - produces discrete srqE mesh

Files *_test: used for testing newly prepared functions/procedures.

Files demo*: working version of tests of different configurations, methods, parameters.

Essential Matlab functions used besides matrix operations in demo* files:
- inv - inverse of the square matrix X
- linsolve - different methods of linear sytem solving (Matlab chooses)
- svd - Singular value decomposition (calculates the diagonal)
- Wiener2 - adaptive noise-removal filtering